Egypt. J. Chem. **Vol. 65, No. 4, pp. 383 - 394 (2022)**

Egyptian Journal of Chemistry

http://ejchem.journals.ekb.eg/

Biosynthesis, Characterization and Analytical Studies of Polymeric Nanoparticles as Adsorbents (AgNPs-IPN's) and their Use for the Removal of Methylene Blue from Industrial Wastewater

Sajda .S. Affat*

**Department of Chemistry, College of Science, University of Thi-Qar, Iraq.*

Abstract

The AgNPs-IPN's has been successfully prepared by synthesized biosynthesis of Ag nanoparticles (AgNPs) from Zizyphus Spina Christi L leaves extract and then linked with polymer network derived from cured epoxy with lignin to produce (AgNPs-IPN's) and characterized by using X-Ray, FTIR, TGA, DTG, SEM, and TEM surface morphology analysis and then used as adsorbent of methylene blue dye from synthetic wastewater. Parameter like pH, contact time, methylene blue concentration, and adsorbent dose concentration was studied. Methylene blue removal increased when the dosage of biosorbent increases. Isotherm adsorption was also described by the Langmuir and Freundleich models, It was found that Langmuir isotherm (R^2 = 0.9956) is better than the Freundlich model (R^2 = 0.9937) which implies that the adsorption of MB on AgNPs-IPN's was monolayer. Thus the maximum adsorption capacities calculated from the Langmuir model was found to be 33.5 $mg.g^{-1}$ and was consistent with the experimental data. The synthesized AgNPs-IPN's showed an excellent activity towards the removal of methylene blue from synthetic wastewater.

Keywords: Methylene blue, AgNPs-IPN's, Nanoparticles, Polymers, Synthetic wastewater

1. Introduction

Dyes and pigments are widely used to colour products, mostly in the textiles, paper, plastics, leather, food, and cosmetic manufacturing. Organic dyes are a fundamental part of many industrial effluents and demand an appropriate method to dispose of them. Chemically, most commercial dyes are stable and difficult to remove from wastewater [1,2]. Methylene Blue (MB) has been selected as a model compound for evaluating the possibility to remove dye from wastewaters. MB is a thiazine (cationic) dye, which is most commonly used for coloring paper, temporary hair colorants, dyeing cotton, wool, and more other uses. Although MB is not considered to be a very toxic dye, it can reveal very harmful effects on living things. After inhalation, symptoms such as difficulties in breathing, vomiting, diarrhea and nausea can occur in humans [3]. Furthermore, over dosage of MB can cause central nervous system toxicity. Because of all these dangers the degradation of MB is environmentally and biologically [4]. These wastewaters are produced in large volumes. This leads to an increase in the complexity of toxic effluents. Therefore, they must be removed before the discharge. However, problems with the aforementioned solutions make it necessary to develop easily available, low-cost, and equally effective alternatives for wastewater treatment. Over the years, a number of technologies have been developed to remove toxicity from wastewater. Many researchers have prepared superabsorbent hydrogels or copolymers based on natural and synthetic polymers for use in the removal of toxicity. The

*Corresponding author e-mail: sajdasabar@gmail.com
Receive Date: 30 August 2021, Revise Date: 16 October 2021, Accept Date: 21 October 2021
DOI: 10.21608/EJCHEM.2021.93443.4413

composites developed by IPN's have exceptional thermal and mechanical characteristics [5,6]. Nanoparticles and nanocomposites have received great attention in materials science because of their small sizes and related unique properties [7,5]. Polymer composites, especially interpenetrating polymer networks (IPN's) have been given more attention in recent years because of their excellent properties, e.g. light weight, high mechanical strength, high wear resistance, good thermal stability, good chemical resistance, etc. [8]. IPNs are polymer alloys made up of two or more polymers arranged in a network form and kept together by permanent entanglements rather than covalent bonds between the chains of the two different types of polymers [9]. When compared to single components, IPN's composites have outstanding thermal stability and mechanical qualities due to the synergetic effect caused by forced compatibility of individual components [5,7]. Green synthesis of nanoparticles has been one of the most attractive areas in nanotechnology for current science research in recent years. Noble metal nanoparticles such as gold, silver, and platinum are widely used in different fields due to their unique size and shape dependent properties [10]. Silver nanoparticles (AgNPs) are the most cost-effective of all noble metal nanoparticles. In addition, AgNPs has optical, catalytic, sensor, antibacterial, and antioxidant properties [9]. The synthesis of AgNPs uses high energy, toxic and expensive chemicals, and poses serious economic and environmental problems. As a result, the purpose of green chemistry is to foster the use of an eco-friendly solvent, reducing and stabilizing agents [12]. Plants and plants extracts have emerged as potential candidate, suitable for large-scale biosynthesis of different nanoparticles. Researchers commented on the advantages of using plants in the creation of nanoparticles which are less expensive, renewable and safe to handle when compared with comparatively costly methods based on microbial processes [13]. In the past few years, there has been an increasing interest in the synthesis of AgNPs using biological systems, including bacteria, fungi, algae and plants have become more significant [14,15]. Green synthesis of AgNPs using plant materials such as stems, leaves, roots, seeds, fruits, and so on has attracted greater attention among the various biogenic approaches due to low cost and gentle experimental conditions without the need for expensive cell culture procedures [16]. Zizyphus spina-christi is locally available, belongs to the Rhamnacea family, and grows wildly in Asia and tropical Africa in Fig.1.

Fig.1. *Zizyphus spina-christi L* leaves

In this study, we explore the biosynthesis of Ag nanoparticles (AgNPs) via a single-step reduction of Ag ions at room temperature without the use of any reducing and/or capping agents using the renewable and biodegradable *Zizyphus spina christi L* leaves extract and linked with polymer network derived from cured epoxy with lignin to produce (AgNPs-IPN's) and using the product to remove methylene blue from synthetic wastewater was evaluated (see Scheme 1).

2. Experimental

2.1 Instrumentation

Thermal analysis was carried out using thermal gravimetry analysis (TGA) (Perkin Elmer-TGA-4000) in College of Science, University of Muthanna at a heating rate of 20°C/min in the temperature range (40-605) under nitrogen atmosphere with a flow rate of 20 ml/min and Differential Scanning Calorimetric (DSC) analysis in the College of Engineering, University of Tehran, at a heating rate of 10°C/min in the temperature range (0-600) under nitrogen atmosphere, The Fourier transform infrared (FT-IR) spectra of the samples were recorded by (Shimadzu, Japan) in the Department of Chemistry College of Science, University of Thi-Qar by KBr disks. The surface morphology was examined from scanning electron microscopy (SEM) and Transmission Electron Microscope (TEM) in College of Engineering, University of Tehran.

2.2 Materials

Silver nitrate ($AgNO_3$,Merck), epoxy resin (DGEBA), lignin, sodium hydroxide (NaOH) and hydrochloric acid (HCl) from (Sigma Aldrich), and methylene blue purchased from (R & M chemicals, UK) were used in this study without further purification.

2.3 Collection, Processing and Preparation of Zizyphus spina Christi Leaf Extract

Fresh *Zizyphus spina christi L* leaves were collected and washed under tap water to remove the adhered and then rinsed with deionized water. The aqueous leaf extract of *Zizyphus spina christi L* was prepared as follows: 25gm of fresh leaves were mixed with 100ml of deionized water in a 250ml flask and the contents were boiled for 10min. The components were cooled to room temperature and filtered through Whatman No.1 filter paper. The clear leaf extract of *Zizyphus spina christi L* this obtained was used for the synthesis of silver nanoparticles [17].

2.4 Synthesis of Silver Nanoparticles

Incubated at room temperature with shacking under dark conditions, 10 ml of 25% *Zizyphus spina christi L* aqueous extract (ZSE) was gradually added into 90 ml of 1mM silver nitrate ($AgNO_3$) in a 250ml conical flask. The reaction solution was checked for 30min. and monitoring for the change in color of the $AgNO_3$ solution from colorless to brown. The AgNPs solution was centrifuged at 15000 rpm for 30min. The supernatant was discarded, and the obtained pellet was re-dispersed in deionized water. The centrifugation for the pellet was repeated two to three times to wash off any substances on the surface of the silver nanoparticles [17].

2.5 Preparation of (AgNPs-IPN's)

The (Ag-nanoparticles/lignin/epoxy) was prepared by mixing Ag–nanoparticles, lignin and epoxy resin (DGEBA) with a weight ratio of (0.1:1:1). Then the temperature was increased up to 50°C with stirring for 90 min by ultrasonic to initiate AgNPs-IPNs polymerization. The product was poured into a glass mold and kept in oven at 70°C for 24hours (Scheme1).

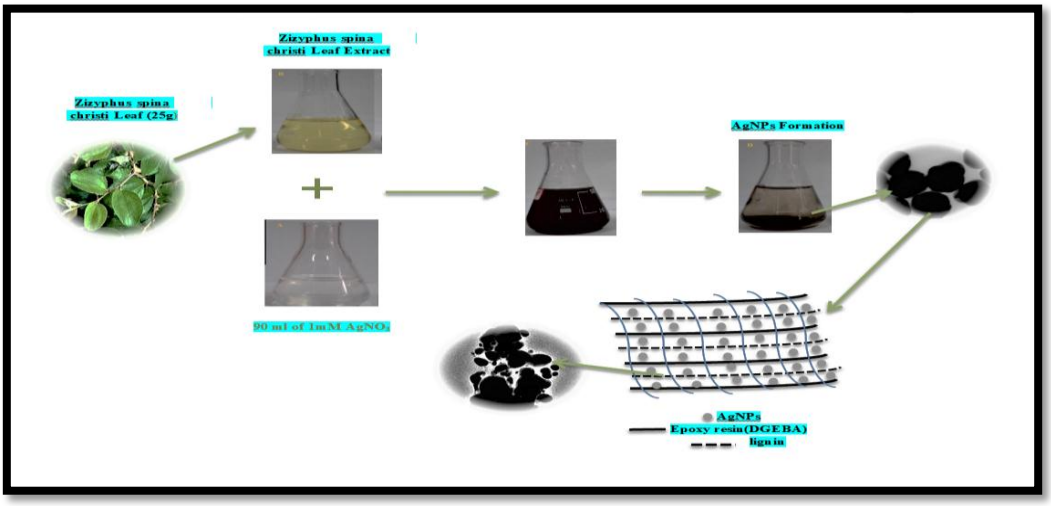

Scheme 1 The bio-synthesis of AgNPs-IPN's

2.6 Adsorption Experiments

In this study, the adsorbent, AgNPs-IPN's, was used to adsorb methylene blue dye from synthetic wastewater. This material was used in the adsorption process without any pre-treatment or modification process. This adsorbent was grained and sieved using (100-200) µm sieves. Methylene blue dye (MW: 319.85, λ max 663nm) was used as the adsorbent. The dye was used directly without any purification. A stock solution was prepared by dissolving 1g of methylene blue dye (99.9%) in distilled water to get a 1000 mg/l stock solution. Then, the stock solutions of methylene blue in the range of 20 to 100 mg/l were prepared to perform the experiments. The pH was modified using sodium hydroxide (0.1MNaOH) and hydrochloric acid (0.1MHCl). The experiments were carried out at constant test laboratory conditions such as the oven temperature of drying (60 ºC), employing the shaker rotation at 180 rpm, centrifugal 3000 rpm, the room temperature of approximately (25ºC).

A specific amount of AgNPs-IPN's (0.1gm mass dosage) was immersed in 100 ml of methylene blue solutions with concentrations of 20, 40, 60, 80, and 100 mg/l in 250 ml conical flasks. The optimum pH was set for each adsorbent and the temperature was 25°C. The amount of dye removal was measured using a UV.Vis Spectrophotometer (Shimadzu, Japan) at a maximum wavelength of 663nm. The time of the experiment was 180 minutes; the dye removal was tested every 10 minutes. The optimum pH was investigated by taking several pH values ranging from 2-10. The 50 mg/l concentration of methylene blue was selected to evaluate the impact of contact time of the adsorption of methylene blue was measured every10 minutes. In this study the dosage of adsorbent was examined by setting the methylene blue dye concentration to 50mg/l. A 100 ml sample was prepared at the optimum pH. The effect of the initial concentration of methylene blue on adsorption rate has been studied by testing concentrations ranging from (20-100) mg/l of methylene blue. All other parameters of the experiment are kept constant [18].

The equilibrium adsorption capacity, q_e (mg/g) and the percentage removal of dye was calculated using the mass balance, according to the following Equations:

$$q_e = (C_o - C_e)\, V/m \quad \text{..... (1)}$$

Where V is of the sample volume (L), m is the mass of the adsorbents (g), C_o is the initial metal ion concentration (mg/l), and C_e is the equilibrium concentration of methylene blue in the solution (mg/l). The concentration of dye removal in solution was measured using UV.Vis [19].

2.7 Study of adsorption isotherms

10 ml of five solutions with concentrations of 20, 40, 60, 80, and 100 mg/l were prepared by proper dilution of stock solution (MB). The optimum conditions of pH, adsorbent dose, adsorbent particle size, agitation speed, temperature, and contact time were adopted according to the sample of adsorbent used for studying adsorption isotherm. At the end, suspensions were filtered off and the filtrates were analyzed for remaining (MB) concentration by using a UV.Vis spectrophotometer. The Langmuir isotherm was plotted by using its standard straight-line Equation (2):

$$\frac{1}{q} = \frac{1}{b q_m c_e} + \frac{1}{q_m} \quad \text{..... (2)}$$

amount of methylene blue adsorbed, C_e (ppm) is the concentration of methylene blue at equilibrium, q_m (mg.g^{-1}) and b (L.g^{-1}) are Langmuir isotherm parameters which were calculated from the slope and intercept values of the linear plot of 1/q versus 1/C_e. The Freundlich isotherm was plotted using the following standard straight-line Equation (3). .

$$\text{Log } q = \text{Log } K_F + \frac{1}{n} \text{Log} C_e \quad \text{..... (3)}$$

The value of K_F can be determined from intercept and 1/n can be determined from the slope of the linear plot of log q versus log C_e. K_F and 1/n are the Freundlich isotherm parameters [20].

3. Results and discussion

3.1 Adsorbent characterization

3.1.1 XRD analysis

The XRD pattern of synthesized AgNPs using *Zizyphus spina christi L* is shown in Fig. 2. There are four major peaks that appear at 38.2°, 44.38°, 64.53° and 77.45°. They were assigned to reflections from the 2 theta region, corresponding to (111), (200), (220) and (311) planes of face-centered-cubic (fcc) geometry of AgNPs, which is in agreement with the JCPDS file No. 42-0783. The maximum intensity came from the (111) plane, which suggests that the synthesized AgNPs are abundantly distributed in the (111) plane [21]. The average crystallite size of AgNPs nanoparticles can be determined from the Debye Scherer formula, Equation (4):

$$D = K\lambda / \beta \cos\theta \quad \text{..... (4)}$$

Where, D is the crystallite size, λ is the wavelength of the X-ray radiation, K is the Scherrer constant, β is the full width at half-maximum height (FWHM), and θ is the Bragg's diffraction angle [22]. Average crystallite size of AgNPs nanoparticles was calculated as 28.559 nm by using full width at half-maximum height (FWHM) of the distinct peaks 2θ° = 43.706, 37.139, 20.332, 13.058.

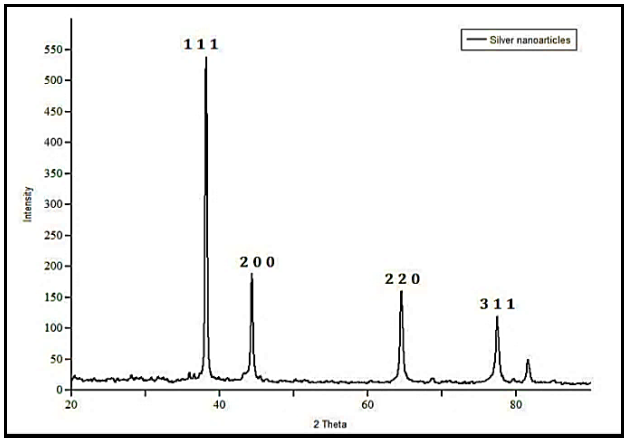

Fig.2. XRD spectra of AgNPs

3.1.2 FTIR analysis

FTIR analysis gives information regarding the chemical transformation of the functional groups involved in the reduction and capping of the metal ions. The FTIR spectra of AgNPs-IPNs are shown in Fig.3. The band at 3398.85cm^{-1} indicates a hydroxyl group (OH) stretching vibration [23,24], the C-H stretching peak appears at 2915.96cm^{-1} and the carbonyl stretching conjugated with the aromatic ring skeleton appears at 1624.18cm^{-1}[25]. The band of epoxy groups at 1041.39 cm^{-1} appears in the spectrum and the band 1368.15cm^{-1} phenolic OH and aliphatic C–H in methyl groups. The aromatic of lignin structure lies in aromatic skeletal vibration in the wavenumber range (1411.83 - 868.80) cm^{-1} [9]. There is also band at 1564.66 cm^{-1} indicating the presence of the C=C group in the aromatic rings [26]. Additional absorption peaks at 1720.43 and 1791.13 cm^{-1} were influenced by the presence of the AgNPs [27,28].

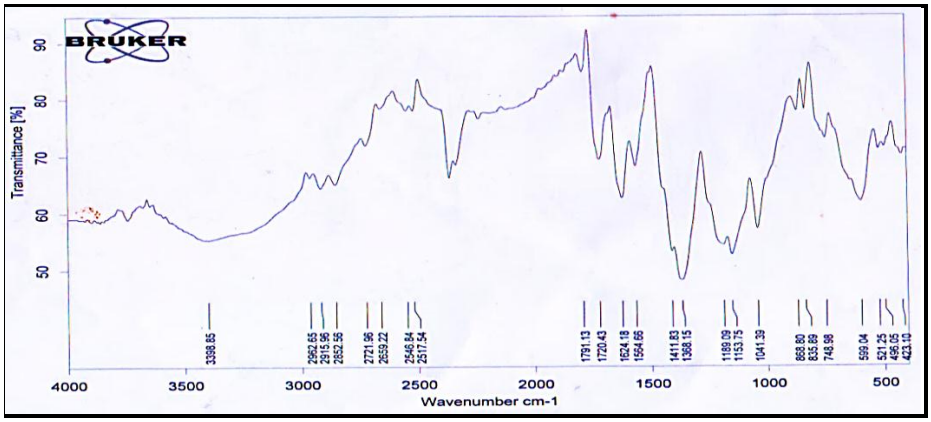

Fig.3. IR spectra of (AgNPs-IPNs)

3.1.3 Thermal studies

The thermal stability of IPNs and Ag-IPNs was evaluated by thermogravimetric analysis (TGA) and differential thermogravimetric (DTG). The TGA and DTG curves of AgNPs-IPNs exhibit higher thermal stability than from IPNs only curves due to the presence of AgNPs, are shown in Fig. 4 (a and b). The TGA and DTG curves for both IPNs and Ag-IPNs show four stages of mass loss. The first stage of mass loss at a temperature above 40°C was related to the removal of moisture and low molecular weight polymeric particles. The second stage of mass loss at temperature above 207°C was assigned to thermal degradation or crosslinking of IPNs and IPNs on the surface of AgNPs in Ag-IPNs. The third stage of mass loss at temperatures above 350°C is due to the decomposition of the polymeric components into volatile water, carbon dioxide and char. Finally, the fourth stage of mass loss a temperatures above 600 °C was associated with the complete degradation of both IPNs and Ag-IPNs. .

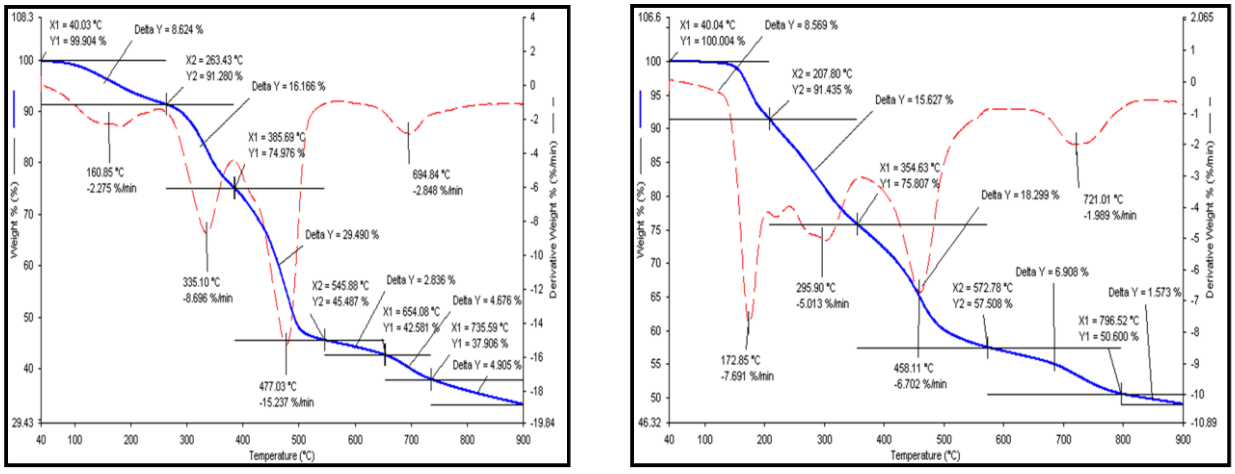

(a) **(b)**

Fig.4. TGA and DTG Curves of (a) IPNs and (b) Ag-IPNs

3.1.4 Surface morphology

The size and morphology structure of (AgNPs-IPN's) was studied by scanning electronic microscopy (SEM) and transmission electron microscopy (TEM). It can be observed that there is a variation in particle sizes from 20 nm to 33 nm (Fig. 5). It was evident that the silver nanoparticles edges were brighter than the center of the nanoparticles, suggesting the particles were encapsulated by IPNs.

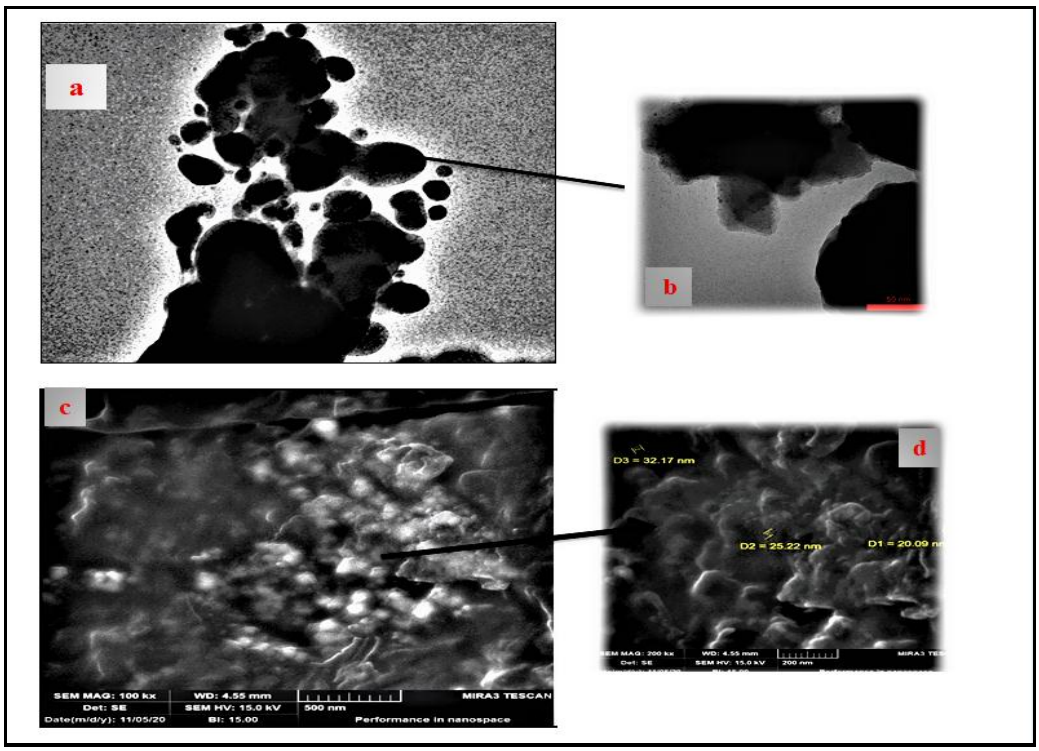

Fig.5. TEM Images (a,b) and SEM Images (c,d) of (Ag NPs-IPN's)

3.2 Adsorption Studies

3.2.1 The effect of pH on removal methylene blue (MB)

The pH of the solution has a significant effect on the adsorption process because it can control the charge of the adsorbent surface, the ionization degree of the pollutants, and structural stability of methylene blue [18]. The variation in the adsorption of methylene blue dye with the initial pH change of AgNPs-IPN's solution was studied in the adsorption of methylene blue and ranged from 2 to 10. Throughout the experiment, 100 ml of dye with initial dye concentration was 50 mg/l of methylene bleu has been investigated with 0.1g of each adsorbent. The percentages of dye removal based on the pH value of the AgNPs-IPN's solution are depicted in Fig. 6. The experiments revealed the optimum pH of treatment solution was found to be equal 8 which resulted in the maximum dye removal. The maximum adsorption efficiency was 96% at pH 8 and this pH value was selected an optimum pH for further studies. Therefore, this value of pH is employed in the followed experiments that were aimed to study the other parameters to ensure the maximum amount of adsorption.

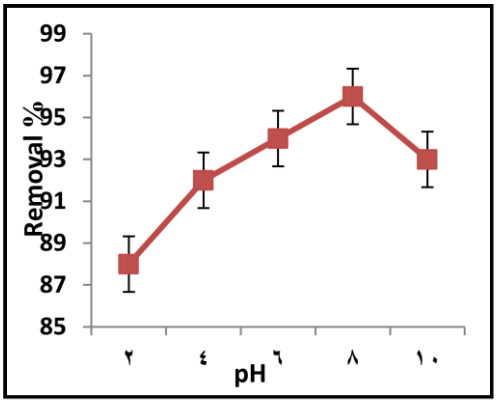

Fig.6. Effect of pH on MB dye removal by AgNPs-IPN's

3.2.2 Effect of time on removal methylene blue (MB)

The efficiency of the adsorption procedure was investigated according to the contact time between dye molecules and the adsorbent. During the adsorption, different data of time have been used till the equilibrium time. Throughout the experiment, 100 ml of dye with an initial dye concentration of 100mg/l of methylene bleu has been investigated with 0.1g of each adsorbent. The optimum pH of the adsorbent has been determined. It is clear that the adsorption of methylene blue rapidly increased with the time increment and then slowed on equilibrium due to more active sites available on the nano polymer (AgNPs-IPN's) and gradually decreased until equilibrium state is reached due to occupancy of active sites of the adsorbent as shown in Fig. 7. It can be seen that the adsorption rate of dye with AgNPs-IPN's showed a dramatic increase in the first 40 minute, whereas the adsorbed amount of dye has been jumped from 88 mg/g at the 50 minute to be 87mg/g. Meanwhile, it kept a steady level after the 60 minutes at 86mg/g. This might be attributed to the availability of the adsorption surface area on the adsorbent particles which is responsible for the rapid adsorption of methylene blue [29]. It was found that the adsorbed amount of dye took about an hour to reach the equilibrium state, which represents the AgNPs-IPNs' maximal adsorption capacity.

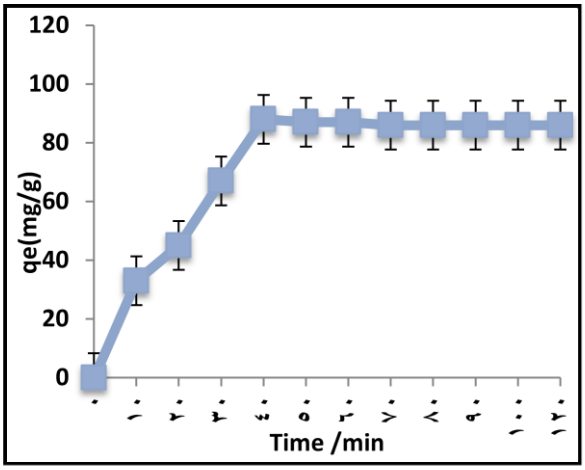

Fig.7. Effect of contact time on removal methylene blue by (AgNPs-IPN's) at pH=8

3.2.3 Effect of initial MB concentration

One of the factors that were assessed in this research is the initial concentration of dye. The Initial concentration is an indicator to identify whether the adsorption process of dye happens in multilayers or monolayers [30]. Five levels of initial concentrations of methylene blue were employed in this study 20, 40, 60, 80, and 100 mg/l at a fixed adsorbent dose which was 0.1gm. All solutions were incubated at 25^0C and shake at 180 rpm for 3 hr. and the time with intervals every 10 minutes. The filtrate samples were collected with the help of a syringe for a spectrophotometric ally absorbance test. As seen in Fig. 8, it can be observed that amount adsorbed at any contact time of adsorption (qt) of methylene blue using the adsorbents AgNPs-IPN's was increased by increasing the concentration of adsorbate, the corresponding adsorption capacity also increases and reaches a maximum at a point where the adsorption remains constant. Fig. 9 shows that increasing the concentration of dye 20 mg/l to 100 mg/l led to increasing the amount of adsorbed dye, qe (mg/g) from 13 to 83mg/g, respectively. The change in the amount removed is attributed to the high mass transfer force of the initial dye concentration which overawed the resistance of mass transfer for molecules between the solid phases and aqueous solution [31].

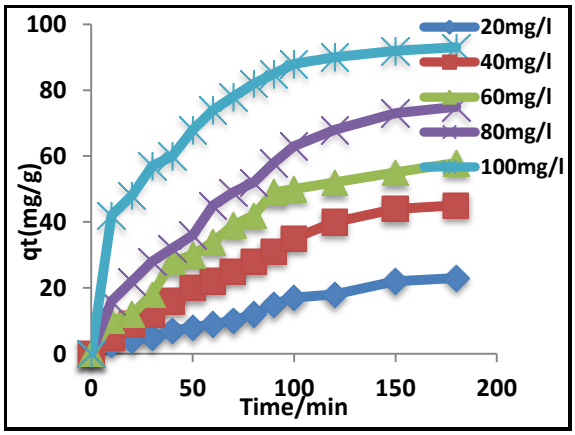

Fig.8. Effect of initial MB concentration for adsorption on AgNPs-IPN's

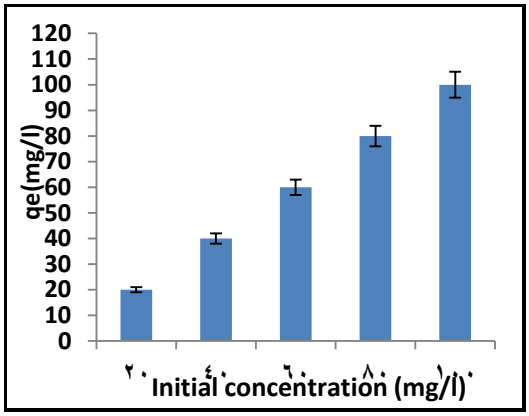

Fig.9. Effect of the initial concentration of MB on adsorption rate

3.2.4 Effect of adsorbent concentration on dye removal

The adsorption of dyes from the aqueous solution can be significantly influenced by the adsorbent dose. Hence, the elevated variation of adsorbent dosage effect was detected at an environment of pH=8 that included a fixed concentration of methylene blue (100 mg/l), 180 rpm, and 25^{o}C till equilibrium time. Fig.10 illustrates the results of removed dye at equilibrium and the percentage of dye removal. The outcomes show that there is an increase in dye removal by increasing the adsorbent dosage, which can be seen in Fig. 10. By the same token, the amount of dye removal was 58.2% using AgNPs-IPN's dosage 0.05gm. It is easy to observe that the dye removal showed a proportional increase in behavior with adsorbent concentration increment. This removal reached a maximum of 94% when the quantity of AgNPs-IPN's dosage was increased to be 0.1 gm.

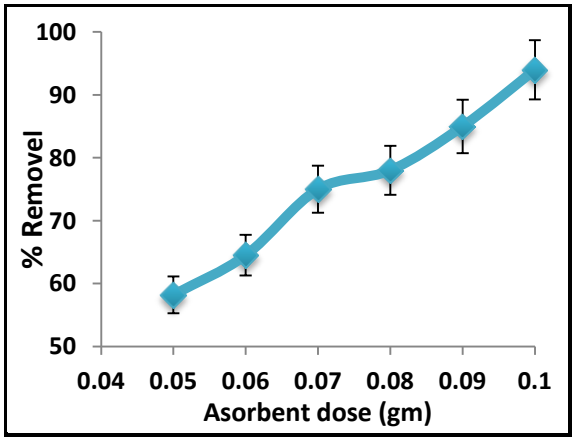

Fig.10. Effect of variation of adsorbent dosage on removal percentage

3.2.5 Adsorption isotherms

Analysis of the adsorption isotherm is important to describe how adsorbate molecules interact with the adsorbent surface and establish the appropriate correlation with the equilibrium curve [32,33]. The Langmuir and Freundlich isotherms were shown graphically in Figs. 11 and 12. The corresponding parameters were listed in Tables 1. According to the coefficients of correlation obtained from linear regression, it was found that in all cases, the Langmuir model fit the data better than the Freundlich model because the correlation coefficients (R_2) values are higher for Langmuir isotherm than for the Freundlich isotherm. This reinforces the fact that the Langmuir isotherm is useful to explain the adsorption of methylene blue (MB) from the solutions on the surface (AgNPs-IPN's) are prepared in this study when it follows the monolayer mode rather than the multilayer mode. A basic assumption of the Langmuir theory is that the sorption can take place at specific homogeneous sites on the adsorption. When a site is occupied by an adsorbate, no further adsorption can take place at that site.

Table1. Parameters of Freundlich and Langmuir constant for Adsorption

Model	Parameter
Langmuir	**Qm (mg.g^{-1}) = 33.5**
	b (L.g^{-1}) = 0.206
	R^2 = 0.9956
Freundlich	**K_F = 1.776**
	1/n = 0.315
	R^2 = 0.9937

Where K_F is the Freundlich parameter associated with the adsorption affinity; is the Freundlich constant and taken as an indicator of adsorption capacity, and 1/n is a measure of the adsorption intensity. If 1/n=1, the adsorption is linear, i.e. the adsorption sites are homogeneous and there is no interaction between the adsorbed species. If 1/n <1, the adsorption is favorable; the adsorption capacity increases and new adsorption sites appear. If 1/n>1, the adsorption is unfavorable; the adsorption bonds become weak and the adsorption capacity decreases [34]. Isotherm model parameters are obtained by determining the slope and intercept or their linear plots (Figs 11and 12), as shown in Table 1. In

order to choose the isotherm model that best describes the experimental data; two comparisons were made based on the R^2. Based on the correlation coefficients, it was possible to conclude that the Langmuir isotherm (R^2 = 0.9956) is the best fit of experimental data than the Freundlich model (R^2 = 0.9937), which implies that the adsorption of MB on AgNPs-IPN's was monolayer. Thus the maximum adsorption capacities calculated from the Langmuir model were found to be 33.5 $mg.g^{-1}$ and were consistent with the experimental data. The maximum adsorption capacities obtained in this study can be compared with other adsorption studies (Table 2).

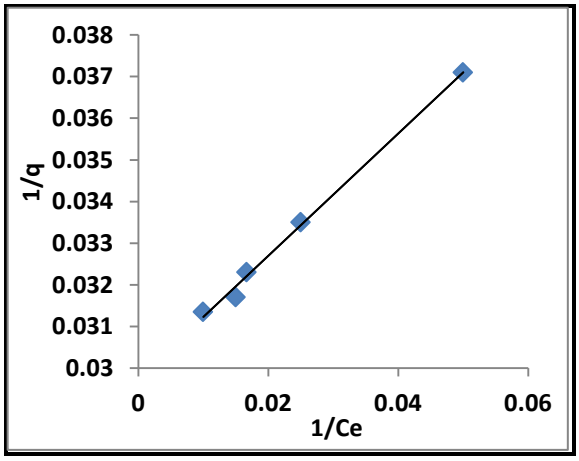

Fig.11. Langmuir adsorption isotherm for MB adsorption by AgNPs-IPN's pH=8, shaking rate 180 rpm, amount of adsorbent 0.1gm)

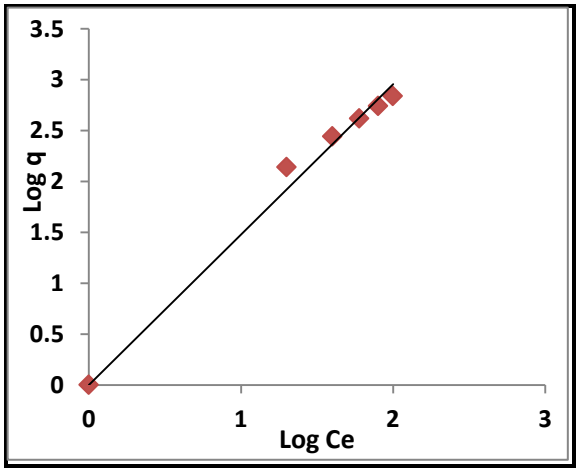

Fig.12. Freundlich adsorption isotherm for MB adsorption by AgNPs-IPN's at (pH=8, shaking rate 180 rpm, amount of adsorbent 0.1gm)

Table2. Comparison of maximum adsorption capacity of AgNPs-IPN's with some other adsorbents

Adsorbent	Q max ($mg.g^{-1}$)	Ref.
Coir pith	5.8	35
Apricot stones	4.133	36
Coconut coir dust	15.25	37
Silk cotton hull	2.40	38
Sago waste	4.51	38
Banana pith	4.67	38
Maize cob	5.00	38
Hazelnut shell	8.82	36
Wheat shell	16.56	39
Tripoli	16.6	40
Raw beech sawdust	9.78	41
Thermally activated coconut activated carbon	20.62	42
Oak saw dust	29.94	43
Raw coconut coir dust	29.50	44
AgNPs-IPN's	33.5	This study

4. Conclusions

Nanopolymerparticles were prepared for Ag in the laboratory using Zizyphus spina christi L leaf extract and $AgNO_3$ to prepare AgNPs, and then linked with polymer network derived from cured epoxy with lignin to produce (AgNPs-IPN's).The AgNPs-IPN's were characterized with X-ray FTIR and UV-Vis, TGA, DTG, SEM and TEM and study adsorption isotherm by the Langmuir and Freundleich models, It was discovered that the Langmuir isotherm (R^2=0.9956) fits the experimental data better than the Freundlich model (R^2=0.9937), implying that MB adsorption on AgNPs-IPNs was monolayer. Thus, the maximum adsorption capacities calculated from the Langmuir model were found to be 33.5 $mg.g^{-1}$ and were consistent with the experimental data, which using the product to remove methylene blue from

synthetic wastewater. The results show the effectiveness of the method used in the preparation of nanoparticles and the stability of the prepared particles and their effectiveness in water purification and environmental remediation. The preparation, of AgNPs-IPN's in this way has several good properties such as high reactivity, easy preparation and low cost compared to other methods of preparation of metal nanoparticles. The synthesized AgNPs-IPN's showed excellent activity towards removal of methylene blue from synthetic wastewater.

5. Conflict of interst:
The author declares no conflict of interest, financial, or otherwise.

6. Formatting of funding sources: Self funding.
7. Acknowledgment: I would like to express my heartfelt thanks to Dr. Asaad Sayer and Dr. Saad Sh. Mohamad for providing assistance with measurements and analysis.

8. References

[1] Nassar, M. M., and Magdy, Y. H., Removal of different basic dyes from aqueous solution by adsorption on palm-fruit bunch particles. *Chem. Eng. J.*, **66**, 223-226 (1997).

[2] Affat, S. S., Classifications, advantages, disadvantages, ral and synthetic Dyes: A review, *University of Thi-Qar Journal of Science*, **8**,130-135 (2021).

[3] Bhattacharya, K.G. and A. Sharma, Kinetics and thermodynamics of methylene blue adsorption on neem (*Azadirachta indica*) leaf powder. *Dyes Pigm.*, **65**, 51-59 (2005).

[4] Gillman, P., K., CNS toxicity involving methylene blue: the exemplar for understanding and predicting drug interactions that precipitate serotonin toxicity. *J Psychopharmacol*, **25**, 429–436 (2011).

[5] Liu, Y. H., He, H. M and Wang, Z. Y., Study on dental plastic IPN post composite. *J Reinf Plast Compos*, **29**, 2684–2690 (2010).

[6] Ramis, X., Cadenato, A. and Morancho, J. M., Polyurethane-unsaturated polyester interpenetrating polymer networks: thermal and dynamic mechanical thermal behavior. *Polymer*,**42**, 9469–9479 (2001).

[7] Tsumura, M., Ando, K., and Kotani, J., Silicon-based interpenetrating polymer networks (IPN's): synthesis and properties, *Macromolecules*, **31**, 2716–2723 (1998).

[8] Cristea, M., Ibanescu, S., and Cascaval, C. N., Dynamic mechanical analysis of polyurethane-epoxy interpenetrating polymer networks. *High Perform Polym*, **21**, 608–623 (2009).

[9] Sperling, L. H., and Mishra, V., The current status of interpenetrating polymer networks. *Polym Eng Sci*, **7**, 197–208 (1996).

[10] Akhtar MS, Panwar J and Yun YS: Biogenic synthesis of metallic nanoparticles by plant extracts. *ACS Sustain.Chem. Eng.*,**1**, 591–602, 2013.

[11] Manjamadha, V. P., and Muthukumar, K., Ultrasound assisted green synthesis of silver nanoparticles using weed plant. *Bioprocess Biosyst. Eng.*, **39**, 401–411 (2016).

[12] Cheviron, P., Gouanve, F., and Espuche, E., Green synthesis of colloid silver nanoparticles and resulting biodegradable starch/silver nanocomposites*Carbohydr Polym.*, **108**, 291–298 (2014).

[13] Rai, M., and Yadav, A., Plants as potential synthesiser of precious metal nanoparticles: progress and prospects. *IET Nanobiotechnol*, **7**, 117-124 (2013).

[14] Balaji, D.S., Basavaraja, S., Deshpande, R., Mahesh, D.B., Prabhakar, B. K., and Venkataraman, A., Extracellular biosynthesis of functionalized silver nanoparticles by strains of Cladosporium cladosporioides fungus. *Colloids Surf., B*, **68**, 88–92 (2009).

[15] Xie, J., Lee, J.Y., Wang, DIC, and Ting, Y.P., Silver nanoplates: from biological to biomimetic synthesis.*ACS Nano*, **1**, 429–439 (2007).

[16] Roy, K., Sarkar, C. K., and Ghosh, C. K., Anticoagulant, thrombolytic and antibacterial activities of Euphorbia acruensis latex-mediated bioengineered silver nanoparticles. *Green Processing and Synthesis*, **8**, 590-599 (2019).

[17] Halawani, E. M., Rapid biosynthesis method and characterization of silver nanoparticles using *Zizyphus spina christi* leaf extract and their antibacterial efficacy in therapeutic

application, *Journal of Biomaterials and Nanobiotehnology*, **8**, 22-35 (2017).

[18] Ethaib, S., and Zubaidi, S.L., Removal of methylene blue dye from aqueous solution using kaolin, *Materials Science and Engineering*, **928,** 022-030 (2020).

[19] Bentahar, S., Dbik, A., El khomri, M., El Messaoudi, N., Bakiz, B., and Lacherai, A., Study of removal of congo red by local natural clay, *St. Cerc. St. CICBIA*, **17**, 295 (2016).

[20] Pragathiswaran, C., Sibi, S., and Sivanesan, P., Low cost adsorbent for heavy metals uptake from aqueous metal ion solution: A review, *International Journal of Research in Pharmacy and Chemistry* **3**(4) (2013).

[21] Zhu, Y., Wang, X., Guo, W., Wang, J., Zhu, C.W., Sonochemical synthesis of silver nanorods by reduction of sliver nitrate in aqueous solution. *Ultrason Sonochem*, **17**, 675–679 (2012).

[22] Edison, TNJI, Atchudan, R., Kamal, C., and Rok, Lee, Y., Caulerpa racemosa: a marine green alga for eco-friendly synthesis of silver nanoparticles and its catalytic degradation of methylene blue, *Bioprocess Biosyst Eng*, **39**,1401-1408 (2016).

[23] Affat, S. S., and Al-Shamkhawy, S. Synthesis and characterization of a 6,6'-((1E,1'E)-(1,2-phenylenebis(azanylylidene))bis(methanylylidene))bis (2-methoxy-3-((6methoxybenzo[d]-thiazol-2-yl)diazenyl)phenol):as a highly sensitive reagent for determination cadmium(II) ion in the real Samples. International Journal of Pharmaceutical Research, 10(4), 480-497 (2018).

[24] Affat, S. S., and Al-Shamkhawy, S. Synthesis, Characterization and spectroscopic studies of a6, 6'- ((1E,1'E)-(1,2-phenylenebis(azanyl-ylidene))bis(methanylylidene))bis(3-(phenyldi-azenyl)phenol)and their complexes. Journal of Global Pharma Technology, 10(10), 207-221(2018). .

[25] Affat, S. S., Hayal, M.Y., and Flifel, I. A., Syntheses, characterization of a new ligand (3 hydrazino-N-isopropylidene-5-methyl-4H-1,2,4- trizole-4-amine) and its complex with (Fe(III), Co(III) and Ni(II)), J.Thi-Qar Sci., 5, 65-71 (2016). [26] Affat, S. S., Synthesis, characterization and theoretical study of Azoimine and using for analysis of palladium (II) Ion by turbidimetric method in environmental samples, Egyptian journal o*f chemistry*, **64**, 5, 2393-2403 (2021).

[27] Rashid, T., Kait, C.F., and Murugesan, T., A Fourier transformed infrared compound study of lignin recovered from a formic acid process, *Procedia Engineering*, **148,** 1312 – 1319 (2016).

[28] Sun, J., Wang, C., Yeo, JCC, Yuan, Du, Hui, Li., and Ludger, P., Stubbs, He Chaobin, Lignin Epoxy Composites: Preparation, Morphology, and Mechanical Propertie, *Macromol. Mater. Eng.*, **301**, 328−336(2016).

[29] Nasuha, N., and Hameed, B.H., Adsorption of methylene blue from aqueous solution onto NaOH-modified rejected tea. *Chemical engineering journal*, **166**, 783-786 (2011).

[30] Ethaib, S., Erabee I.K, Abdulsahib A.A., Removal of Methylene Blue Dye from Synthetic Wastewater using Kenaf Core and Activated Carbon, *International Journal of Engineering & Technology*, **7**, 909-913 (2018).

[31] Ho, Y.S., Chiu, W.T., and Wang, C.C., Regression analysis for the sorption isotherms of basic dyes on sugarcane dust. *Bioresource technology*, **96,** 1285-1291 (2005).

[32] Crini, G., Gimbert, F., Robert, C., The removal of Basic Blue 3 from aqueous solutions by chitosan-based adsorbent: Batch studies. *Journal of Hazardous Materials*, **153**, 96–106 (2008).

[33] Daneshvar, E., Sohrabi, M.S., Kousha, M., Shrimp shell as an efficient bioadsorbent for Acid Blue 25 dye removal from aqueous solution. *Journal of the Taiwan Institute of Chemical Engineers*, **45**, 2926–2934 (2014).

[34] Güzel, F., Saygili, H., Saygili, G.A., and Koyuncu, F., Elimination of anionic dye by using nanoporous carbon prepared from an industrial biowaste, *Journal of Molecular Liquids*, **194**, 130-140 (2014).

[35] Kavitha, D., and Namasivayam, C., Experimental and kinetic studies on methylene blue adsorption by coir pith carbon, *Bioresource Technology*, **98**, 14–21 (2007).

[36] Aygün, A., Yenisoy-Karakaş, S., and Duman, I., Production of granular activated carbon from fruit stones and nutshells and evaluation of their physical, chemical and adsorption properties, *Microporous and Mesoporous Materials*, **66**, 189–195 (2003).

[37] Macedo, J.S., Júnior, N.B., and Almeida, L.E., Kinetic and calorimetric study of the adsorption of dyes on mesoporous activated carbon prepared from coconut coir dust, *Journal of Colloid and Interface Science*, **298**, 515–522 (2006).

[38] Kadirvelu, K., Kavipriya., M., Karthika Radhika, M., Vennilamani, N., and Pattabhi, S., Utilization of various agricultural wastes for activated carbon preparation and application for the removal of dyes and metal ions from aqueous solutions," *Bioresource Technology*, **87**, 129–132, (2003).

[39] Bulut, Y., and Aydin, H., A kinetics and thermodynamics study of methylene blue adsorption on wheat shells. *Desalination*, **194**, 259–267 (2006).

[40] ALzaydien, A.S., Adsorption of methylene blue from aqueous solution onto a low-cost natural jordanian tripoli, *American Journal of Applied Sciences*, **6**, 1047-1058 (2009).

[41] Franca, A. S., Oliveira, L.S., Ferreira, M.E., Kinetics and equilibrium studies of methylene blue adsorption by spent coffee grounds. *Desalination*, **249**, 267–272 (2009).

[42] Sharma, Y.C., and Uma, S.N., Removal of a cationic dye from wastewaters by adsorption on activated carbon developed from coconut coir. *Energy Fuels*, **23**, 2983–2988 (2009).

[43] Ferrero, F., Dye removal by low cost adsorbents: hazelnut shells in comparison with wood sawdust. *Journal of Hazardous Materials*, **142**, 144–152 (2007).

[44] Etim, U. J., Umoren, S. A., and Eduok, U. M., Coconut coir dust as a low cost adsorbent for the removal of cationic dye from aqueous solution, *Journal of Saudi Chemical Society*, **20**, S67-S76 (2016).